

Satellite-and Ground-Based Red Tide Detection Method and System by Means of Peak Shift of Remote Sensing Reflectance

Kohei Arai

Information Science Department
Saga University
Saga City, 840-8502, Japan

arai@is.saga-u.ac.jp

Yasunori Terayama

Information Science Department
Saga University
Saga City, 840-8502, Japan

terra@is.saga-u.ac.jp

Abstract

A method for detection of red tide by means of remote sensing reflectance peak shift is proposed together with suspended solid influence eliminations. Although remote sensing reflectance peak is situated at around 550nm for sea water without suffered from red tide, the peak is shifted to the longer wavelength when sea water is suffered from red tide. Based on this fact, it is capable to detect red tide using high wavelength resolution of spectroradiometers. The proposed system uses green color filtered cameras. Acquired imagery data can be transmitted through wireless LAN to Internet terminal and can be archived in server through Internet. This is the proposed ground based red tide monitoring system. The paper also proposes a method for removing suspended solid influence on red tide suffered area estimations. The proposed method and system is validated in laboratory and field experiments. The system is deployed at coastal areas of the Ariake Sea in Kyushu, Japan.

Keywords: Red Tide, Remote Sensing Reflectance, MODIS, Sensor Network.

1. INTRODUCTION

In accordance with increasing of phytoplankton concentration, sea surface color changes from blue to green as well as to red or brown depending on the majority of phytoplankton (Dierssen et al, 2006) so that it is capable to detect red tide using this color changes [1]. It is also possible to detect red tide using Moderate Resolution Imaging Spectroradiometer: MODIS ocean color bands data. Almost more than 90 % of reflected radiance in the visible to near infrared wavelength region from the ocean is derived from the atmosphere so that atmospheric correction is needed before red tide detection. An iterative approach (Arnone et al., 1998 [2]; Stumpf et al., 2003 [3]) for sediment-rich waters, based on the Gordon and Wang (1994) algorithm [4], is used to correct for the atmospheric interference in the six ocean color bands of MODIS in turbid coastal waters to obtain water leaving radiance, which are then used in the band-ratio algorithm (O'Reilly et al., 2000 [5]) to estimate Chlorophyll in unit of mg m^{-3} . Also suspended solid is estimated with two bands algorithm (visible minus near infrared bands data). The multi-channels of red tide detection algorithms (in the formula of $C=(R_i-R_j)/(R_k-R_l)$ where R_i , R_j , R_k and R_l are the reflectivity derived from bands i , j , k and l .) are proposed. Also learning approaches based on k-nearest neighbors, random forests and support vector machines have been proposed for red tide detection with MODIS satellite images (Weijian C., et al., 2009) [6].

One of the problems on the conventional satellite imagery data based red tide detection methods is that detection accuracy is not good enough followed by elimination of influence due to suspended solid from the detected red tide. The procedure of the proposed method is to estimate red tide index C together with suspended solid first, then remove the influence due to suspended solid from the estimated red tide index by comparing both. Atmospheric correction is out of scope

of the paper because there are atmospheric corrected MODIS data products. The proposed method is based on the multi-channels of red tide detecting algorithm with suspended solid influence eliminations.

The paper also proposes ground based red tide monitoring system. The system uses camera data with green color filter. Red tide contaminated sea water shows remote sensing reflectance wavelength peak shift so that camera data with green color filter of red tide contaminated sea are shows a little bit higher radiance rather than that of just sea water without contamination. Acquired camera data is transmitted through wireless LAN (local Area Network) and Internet. This is a ground based measurement system which allows red tide detection even in the cloudy and rainy weather conditions; satellite imagery data based method does not work in such weather conditions.

The following section describes the proposed method followed by some experimental results. The final section describes conclusions and some discussions.

2. THE PROPOSED RED TIDE DETECTION METHOD AND SYSTEM

2.1 Method for Red Tide Detection With MODIS Data

The multiband ratio algorithms for red tide detection is expressed as follows,

$$C = (R_i - R_j) / (R_k - R_l) \tag{1}$$

where R_i , R_j , R_k and R_l are the reflectivity derived from bands i , j , k and l . If $C \geq t$, then the pixel is assumed to be red tide suffered, where t is a threshold. It is expressed with MODIS bands 8, 10, and 12 (See Table 1) as follows,

$$C = (R_8 - R_{10}) / (R_{12} - R_{10}) \tag{2}$$

MODIS Band 8	405 – 420nm	Radiance 44.9	S/N ratio 880
9	438 - 448	41.9	838
10	483 - 493	32.1	802
11	526 - 536	27.9	754
12	546 - 556	21.0	750
13	662 - 672	9.5	910
14	673 - 683	8.7	1087
15	743 - 753	10.2	586
16	862 - 877	6.2	516

TABLE 1: Wavelength coverage of MODIS (Ocean channels)

Chlorophyll, pigments, fatty acids, total suspended solids, sediments, and Color Dissolved Organic Matter: CDOM absorption is closely related each other. In particular, it is used to occur red tide is detected together with suspended solids. Suspended solids influence on red tide detection has to be eliminated from the calculation of C. Suspended solid can be expressed as follows,

$$\ln(S) = VIS - NIR \tag{3}$$

where *VIS* and *NIR* denotes visible band data and near infrared band data, respectively. MODIS bands 9 and 16 are selected for visible and near infrared channels of data, respectively. Absorption coefficients at the wavelength of 440nm is proportional to *S* so that *S* can be calculated with MODIS band 9 data, *M₉* based on the following equation,

$$S = C_1 - C_2 M_9 \tag{4}$$

where *C_i* is regressive coefficients. *C_i* can be determined through a regression analysis. Also, equation (5) is used for the regression analysis.

$$\ln(C_1) = C_0(M_9 - M_{16}) \ln(C_2 M_9) \tag{5}$$

Then detected red tide pattern is compared to the suspended solid pattern for compensation of suspended solid influences on red tide detections.

2.2 Red Tide Monitoring System With Camera Data With Green Color Filter

Figure 1 shows the proposed red tide monitoring system with the band-pass filter (@550nm) attached web camera together with water quality measuring instruments as well as meteorological data collection robot.

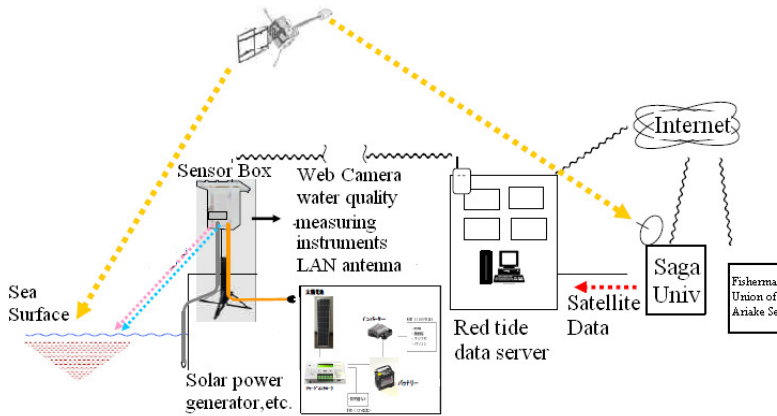


FIGURE 1: The proposed red tide monitoring system with the band-pass filter attached web camera together with water quality measuring instruments as well as meteorological data collection robot

Due to the fact that remote sensing reflectance peak is shifted to longer wavelength than 550nm for red tide suffered sea water, the band-pass filtered (550nm) camera data might be possible to indicate existence of red tide. Figure 2 shows a set of example of the spectral reflectance of normal and red tide contaminated sea surfaces.

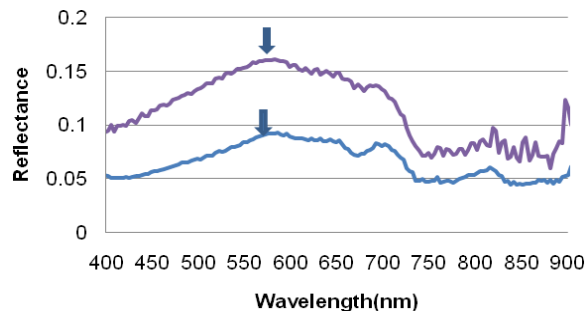


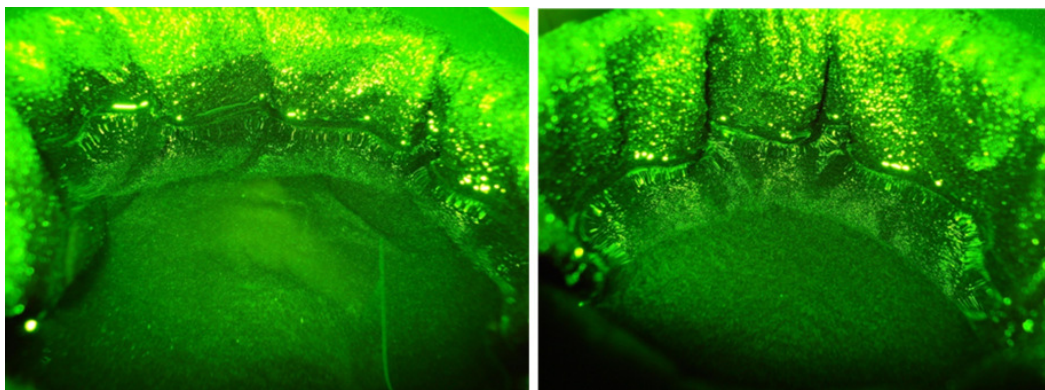
FIGURE 2: Sea surface reflectance measured at the Nanaura in Kyushu, Japan on April 20 (top: normal condition) and August 10 (bottom: red tide contaminated) 2010

The peak spectrum of red tide contaminated sea surface (August 10) is a little bit longer than that of normal condition of sea surface (April 20). Therefore, it is possible to detect red tide using green filtered camera imagery data.

3. EXPERIMENTS

3.1 Camera data with green color filter

Camera data with green color filter of *Chattonella Antiqua* containing water and just water are acquired together with histograms. The results are shown in Figure 3 and 4, respectively.



(a) *Chattonella Antiqua* containing water

(b) Just water

FIGURE 3: Camera data with green color filter of *Chattonella Antiqua* containing water and just water

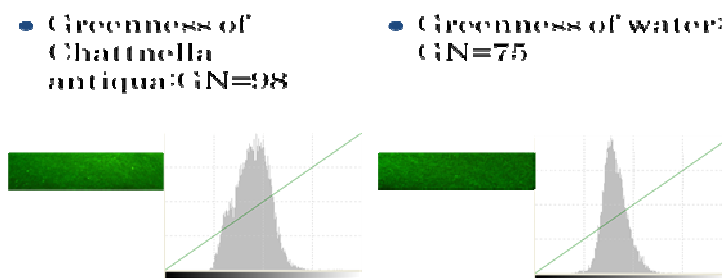


FIGURE 4: Histogram of the camera data with green color filter of *Chattonella Antiqua* containing water and just water

Also camera data with green color filter are acquired in the field at the Nanaura coast in the Ariake Sea, Kyushu, Japan on the different days. Figure 5 and 6 shows the results. There are so many red tide events in the period as follows,

May 21: *Heterosigma*:10, *Skeletonema* spp.:7125

June 25: *Heterosigma*:100, *Skeletonema* spp.:6450→**G=160**

July 5: *Chattonella Antiqua*:480, *Chattonella* spp.:130

July 20: *Skeletonema* spp.:88000→**G=175**

August 2: *Crypt*: 18000

August 10: *Chattonella Antiqua*:1080→**G=140**

August 17: *Thalassiora* spp.:6000, *Skeletonema* spp.:7250, *Chattonella* spp.:1400→**G=120**

November 22: *Akasiwo sanguinea*: 640→**G=125**

The number after the name of red tide type denotes the number of counted red tide while G denotes the average of the camera data with green color filter. Both the insitu data of the number of red tide provided by the Saga Prefectural Ariake Fishery Promotion Center: SPAFPC and the average of camera data with green color filter show a good correlation and coincidence.



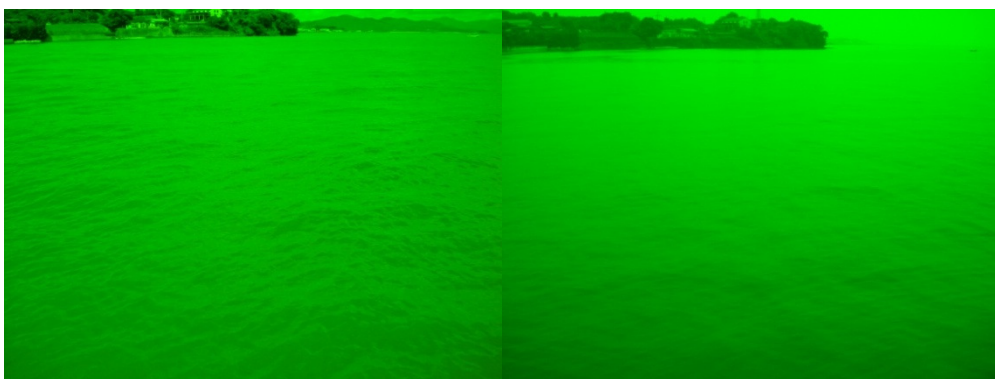
(a) June 23

(b) July 25



(c) August 10

(d) August 26



(e) September 11

(f) September 27



(g) October 23

(h) November 14

FIGURE 5: Camera data with green color filter of the Nanaura sea surface at the Ariake Sea in Kyushu, Japan on the different days in 2010.

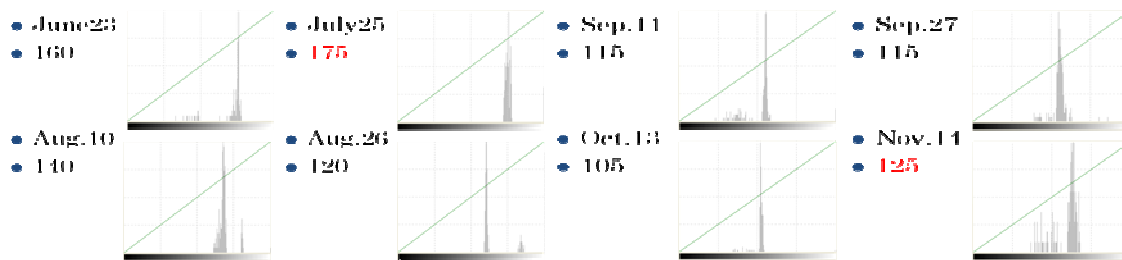
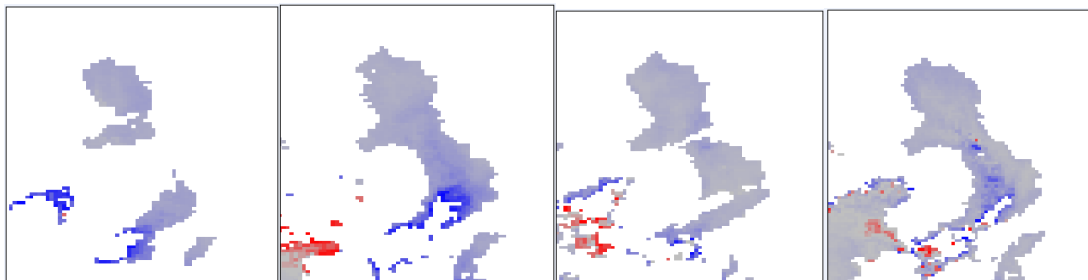


FIGURE 6: Histograms of the acquired camera data with green color filter of the different days.

3.2 MODIS Based Red Tide Index, C

Figure 7 shows MODIS based red tide index C together with red tide events provided by SPAFPC.



(a) 2010/05/1

(b) 2010/05/17

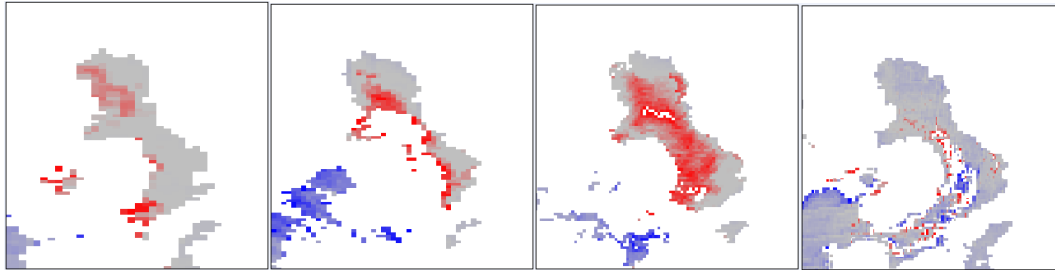
(c) 2010/06/02

(d) 2010/06/09

May 21: Heterosigma:10 Skeletonema spp.:7125,

June 25: Heterosigma:100, Skeletonema spp.:6450,

July 5: Chattonella Antiqua:480, Chattonella spp.:130, July 20: Skeletonema spp.:88000



(e) 2010/07/20 (f) 2010/08/06 (g) 2010/08/18 (h) 2010/11/20
 August 2: *Cryptosporidium*:18000, August 17: *Thalassiosira* spp.:6000, November 22: *Akashiwo sanguinea*: 640

FIGURE 7: MODIS based red tide index C together with red tide events provided by SPAFPC.

In Figure 7, the MODIS based red tide index, C is quantized with two bits so that the data is represented with white, grey blue and red of pseudo colors. In particular, white pixels are contaminated with clouds. Red color pixels shows red tide suffered areas. In the beginning of July, *Chattonella Antiqua* type of red tide appeared then red tide suffered areas is getting large until August 20. After that, red tide disappeared rapidly. In the late of November, the different type of red tide appeared. The MODIS based red tide index, C shows totally identical to the red tide warning report from SPAFPC.

3.2 Suspended Solid Derived from MODIS

Based on the equation (4), suspended solid is estimated. Through correlation analysis, 667nm of MODIS band shows the highest correlation so that linear regression with MODIS band 13 and insitu data of S measured at the observation tower in the center portion of the Ariake Sea is conducted. Equation (6) shows regressive equation. Table 2 shows the match-up dataset between both.

$$S = \alpha * [Lw(667)]N + \beta \quad (6)$$

Observation Date	412	443	531	667	S
2010/06/02 11:00	0.5549	0.758	1.6932	0.5243	3.2
2010/06/03 12:00	0.697	0.7029	1.5953	0.5707	3
2010/06/09 11:00	0.8175	1.0853	2.0067	0.7259	7.7
2010/07/20 11:00	0.2687	0.3801	1.3053	0.5695	7
2010/07/20 14:00	0.3707	0.3684	0.7593	0.2527	4.1
2010/07/21 13:00	0.4012	0.2148	0.6054	0.1987	4.9
2010/07/22 13:00	0.7987	1.0449	1.984	0.9338	4.5
2010/07/23 13:00	1.0671	1.3122	2.3904	1.4277	10.3
2010/8/6 11:35	0.7874	0.5541	1.2454	0.5381	2.7
2010/8/6 13:10	0.5967	0.5353	1.1487	0.4942	3.1
2010/8/18 13:35	0.5477	0.513	1.0888	0.453	2.5
2010/8/19 11:00	0.6398	0.727	1.7675	0.8588	3.6
2010/8/21 10:50	0.2006	0.2884	0.936	0.2832	2.4
2010/8/21 14:00	0.3947	0.5356	0.9892	0.2442	2.4
2010/8/22 13:10	0.8374	0.8131	1.4261	0.6707	3.6
2010/8/23 13:55	0.5518	0.6825	1.5094	1.0073	11.4
2010/8/25 13:40	0.6758	0.866	1.7356	1.1435	11.9

TABLE 2: The data used for regressive analysis, relation between xxx(nm) channels of MODIS data and insitu data of S (mg m^{-3}) measured at observation tower situated in the center portion of the Ariake Sea

Then the following regressive coefficients and Root Mean Square Error is estimated $\alpha = 7.0948$, $\beta = 0.6463$, $\text{RMSE} = 2.08758$. Using the regressive equation, S is calculated. Some examples of S are shown in Figure 8.

After all, it is possible to remove the same pattern of river water, in particular, from the estimated red tide index, C. Although the estimated red tide index used to show river water pattern, it can be removed using the river water pattern estimated with the regressive equation. Thus an influence due to suspended solid is removed.

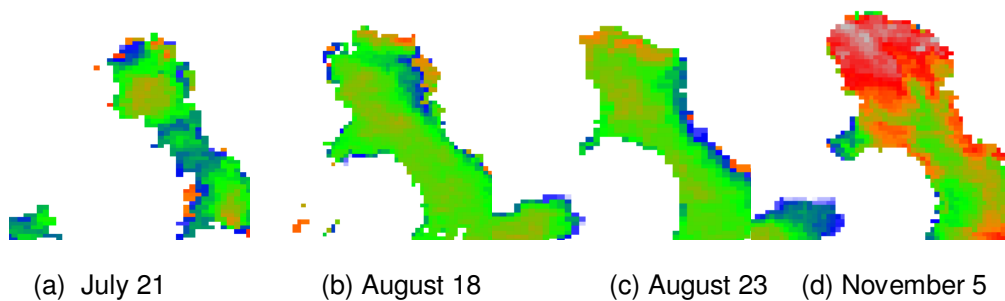


FIGURE 8: Estimated suspended solid pattern derived from the regressive equation

4. CONCLUSIONS

It is confirmed that the proposed method and system for red tide monitoring with camera data with green color filter is effective through laboratory based and at the test site in the field of the Ariake Sea, Kyushu, Japan. Also the proposed method of influence removal due to suspended solid on red tide index measurement with MODIS type of remote sensing imagery data is validated.

5. ACKNOWLEDGEMENT

This research is founded by the Ministry of Education, Culture, Sports, Science and Technology, MEXT Japan so that the authors would like to thank to staff of the space utilization promotion program under the MEXT. Also the authors would like to thank to Dr. Kawamura and Dr. Matsubara of Saga Prefectural Ariake Fishery Promotion Center for their valuable comments and suggestions together with Associate Professor Dr. Katano of Institute of Lowland and Marine Science, Saga University for his nice discussions and providing the Chattonella Antique and marina containing water.

6. REFERENCES

- [1] Dierssen H.M., R.M.Kudela, J.P.Ryan, R.C.Zimmerman, Red and black tides: Quantitative analysis of water-leaving radiance and perceived color for phytoplankton, colored dissolved organic matter, and suspended sediments, *Limnol. Oceanogr.*, 51(6), 2646–2659, E 2006, by the American Society of Limnology and Oceanography, Inc., 2006.
- [2] Arnone, R. A., Martinolich, P., Gould, R. W., Jr., Stumpf, R., & Ladner, S., Coastal optical properties using SeaWiFS. *Ocean Optics XIV*, Kailua Kona, Hawaii, USA, November 10–13, 1998. SPIE Proceedings., 1998.
- [3] Stumpf, R. P., Arnone, R. A., Gould Jr., R. W., Martinolich, P. M., & Martinolich, V., A partially coupled ocean-atmosphere model for retrieval of water-leaving radiance from SeaWiFS in coastal waters. In S. B. Hooker, & E. R. Firestone (Eds.), *SeaWiFS Postlaunch Tech. Report Series. NASA Technical Memorandum*, 2003-206892, vol. 22 (p. 74), 2003.
- [4] Gordon, H. R., & Wang, M., Retrieval of water-leaving radiance and aerosol optical thickness over the oceans with SeaWiFS: A preliminary algorithm. *Applied Optics*, 33, 443–452, 1994.
- [5] O'Reilly, J. E., Maritorena, S., Siegel, D. A., O'Brien, M. C., Toole, D., Chavez, F. P., et al., Ocean color chlorophyll a algorithms for SeaWiFS, OC2, and OC4: Version 4. In B. Hooker, & R. Firestone (Eds.), *SeaWiFS Postlaunch Tech. Report Series. NASA Technical Memorandum* 2000-206892, vol. 11 (p. 2000), 2000.
- [6] Weijian C., Hall, L.O., Goldgof, D.B., Soto, I.M., Chuanmin H, Automatic red tide detection from MODIS satellite images, *Systems, Man and Cybernetics*, 2009. SMC 2009. IEEE International Conference on SMC, 2009.
- [7] Kohei Arai and Yasunori Terayama, Polarized radiance from red tide, *Proceedings of the SPIE Asia Pacific Remote Sensing*, AE10-AE101-14, Invited Paper, 2010
- [8] Kohei Arai, *Red tides: combining satellite- and ground-based detection*. 29 January 2011, *SPIE Newsroom*. DOI: 10.1117/2.1201012.003267, <http://spie.org/x44134.xml?ArticleID=x44134>